Preprints of the 21st IFAC World Congress (Virtual)
Berlin, Germany, July 12-17, 2020

Pinning-based Distributed Predictive Control of Secondary Voltage for an Islanded Microgrid

Yi Yu * **Guo-Ping Liu** *,** **Wenshan Hu** * **Hong Zhou** *

* *School of Electrical Engineering and Automation, Wuhan University, Wuhan, 430072, China, (e-mail: yiyu.py@whu.edu.cn)*
** *School of Engineering, University of South Wales, Pontypridd CF37 1DL, U.K., (e-mail: guoping.liu@whu.edu.cn)*

Abstract: In this study, a pinning-based distributed predictive control of secondary voltage is proposed for an autonomous microgrid (MG) with communication constraints. The proposed predictive control is fully distributed, which requires the information of each distributed generator (DG) on an islanded microgrid and that of its neighbors. In particular, the predictive control scheme can compensate for the communication constraints actively rather than passively. Moreover, it could reduce the computation burden of the controller owing to the developed pinning-based control scheme. It is worthwhile to mention that the purpose of voltage restoration based on distributed predictive control is achieved by minimization of the utility function, which not only ensures the feasibility of the control input but also restores the voltage of an autonomous microgrid to a prescribed level simultaneously through an introduction of tracking and coordination cost. Finally, simulation results are presented to validate the effectiveness of the proposed control methodology.

Keywords: Distributed predictive control, islanded microgrid, pinning control, communication delays.

1. INTRODUCTION

With the growing concerns on the environment, more renewable energy resources (RERs) have been adopted in industry and living supplies. Another main reason for the introduction of RERs is that it is inexhaustible and economical for supplying electric power to the remote district. The power systems that integrate varieties of RERs are called microgrids. A microgrid can operate in grid-connected and islanded modes. Generally speaking, a grid-connected MG means that it is connected with the power grid, whose dynamic characteristics obey the assigned control command of the big grid and without being dominant by any other control. Therefore a MG operating in this mode is similar to an energy storage device or a load, which imposes no challenges of grid control. However, a MG operating in the islanded mode needs to be controlled artificially for stable operation and reliable power outputs. Moreover, the inertia of an islanded MG is too small inertia to consider, comparing with that of the big grid. In this case, the small power system is very sensitive to disturbances and load changes. Hence it is crucial to develop valid control strategies for the islanded MG system.

To form a microgrid for the grid connection of local distributed generators, the hierarchical control scheme is a commonly adopted framework (Guerrero et al., 2011), which generally consists of primary control, secondary control, and tertiary control. Droop control algorithms that respond quickly without relying on communication plays the role of primary control, which mimics the parallel operation characteristics of synchronous generators (Zhong and Weiss, 2011). However, droop control can result in voltage and frequency deviations between the output and the reference values, which may not generally be within the permitted range. Therefore, secondary control is demanded to eliminate the deviations. At present, a large body of literature (Bidram et al., 2013, Lu et al., 2018, Aryani and Song, 2019) studies the voltage and frequency secondary control of MG based on the theory of multi-agent consensus, which realizes the interconnection of multiple DGs in this stage. In the cooperative secondary control framework, distributed controllers usually collect the operation and status information of neighboring DGs through the network to adjust their own power generation behaviors. This control scheme can be efficient and robust. Obviously, the communication system plays a crucial role in the cooperative control of microgrid outputs. However, once the communication system is introduced, no matter wired communication or wireless communication, or even with the currently most advanced 5G communication techniques, communication constraints are ubiquitously caused by the limits of bandwidth, traffic congestions et.al. Therefore, considering the reliability of MG, it is necessary to study the voltage and frequency synchronization of microgrid with communication constraints using cooperative control theory. Many efforts have been devoted to this topic (Lai et al., 2019, Zhang and Hredzak, 2019).

⋆ This work was supported in part by the National Natural Science Foundation of China under Grants 61773144 and 61690212.

Zhang and Hredzak (2019) proposed the cooperative voltage finite-time control strategy with the discovered global information, which deploys primary and secondary voltage control, to achieve voltage restoration on DC microgrids with communication constraints. Although many of them have been struggling to address voltage and frequency synchronization problems for the time-delayed microgrid system, the results obtained are relatively conservative, and some higher-order controllers are difficult to realize in the actual power grid. Unfortunately, to the best of our knowledge, few works have proposed the control method to initiatively compensate for the time delay and data loss during communications, so far. Therefore, for large-scale networked control systems like MGs, if time delays and data loss, are compensated actively, not only the stability and security of such a power system can achieve significant improvements but also the advantages of the cyber network can be maximized. Motivated by these observations, a distributed predictive control method is proposed in this paper which will be able to actively compensate for these constraints encountered in the communication on an inverter-based isolated MG. In addition, the proposed control is different from traditional model predictive control (Liu, 2018), in which the observer-based state-feedback control method was employed. Under this framework, the reference information is not required for all DGs, but only be available for several or even one selected node called a pining node. Accordingly, when the microgrid reference information changes, only that of the pining nodes need an update, instead of each network node, which makes great sense for the large-scale MG systems. To sum up, the main contribution of this paper is to propose a novel pinning-based distributed predictive control to solve the voltage restoration problems on a MG with communication constraints. What's more, under this control strategy, microgrid posses not only the robustness to communication constraints but also plug and play capability, which can meet the requirements of grid connection or off-grid of each DG at any time without affecting the operational stability of the MG.

2. SYSTEM STRUCTURE AND PROBLEM STATEMENT

2.1 System structure

For an autonomous operational microgrid, the standard framework in the literature is to model an inverter as a controlled voltage source behind a reactance. In this case, hierarchical control is widely adopted in the microgrid field, which includes primary control, secondary control, and tertiary control. Besides, there are local inverter internal control loops including voltage and current controllers, which are designed to reject high-frequency disturbances and circle current. Assuming the MG line is highly inductive, the fastest response is the power control. In this stage, the power generation unit would immediately adjust the power output via voltage and frequency according to their respective droop coefficient, which shows the $Q-V$, $P-f$ droop characteristics. Nevertheless, if secondary control exists, it will work on a larger time scale comparing with primary control, to compensate for the deviation caused by droop control. Under the composite drive of primary and secondary controls, the voltage and frequency of each DG will synchronize to the specified value. Then, the output LC filter and coupling inductor are served as the power processing section connecting DGs to form a microgrid. All in all, the inverter-based microgrid architecture includes the power controller, output filter, coupling inductor, and inner control loops, which are shown in Fig. 1.

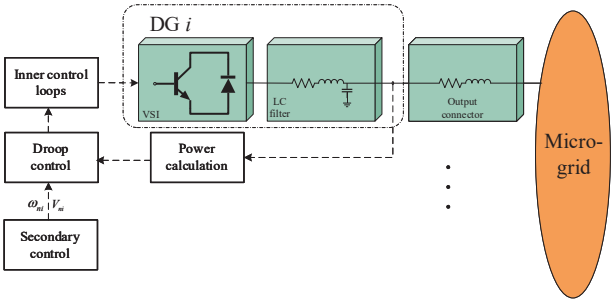

Fig. 1. Block diagram of an inverter-based DG

2.2 Problem statement

Based on the microgrid structure shown in Fig. 1, a decentralized control method will be designed in this paper to maintain the output voltage of islanded microgrid to a rated level. Therefore, the secondary distributed voltage control requires a communication layer compared with primary control, which would make a great significance for the improvement of the operation stability and flexibility of islanded microgrid and can endow microgrid with plug-and-play capability. Under the distributed control scheme, apart from its own operation information, each DG controller can also receive the operation information of the neighboring DGs, further obtains the control signals according to the information received. The control inputs adjust the outputs to realize the voltage recovery and synchronization of each node in the network, so as to achieve the grid-connection of the microgrid. Therefore, it is assumed that DGs can communicate with each other through a cyber network described by a digraph. The digraph is usually expressed as a triples set $G=(V_g, E_g, A_g)$ with a finite set of N nodes $V_g=\{v_1, v_2, \ldots, v_N\}$, a set of edges E_g, and associated adjacency matrix $A_g=[a_{ij}]$, where each node represents a DG unit interfaced via an inverter in the physical layer and interlinked via E_g in the cyber layer. However, for actual networked microgrid systems, based on whether wired or wireless communication, there exist a variety of communication constraints, including network delays, packet dropouts, attacks, etc. This paper aims to consider a distributed secondary voltage control under network delay and packet dropouts, which are the main constraints in communication systems. In the purpose to simplify design of the distributed controller, the following assumptions are made for the microgrid system on the premise of conforming to the actual operation condition of the power grid. Assumptions: (1) The topology of the communication network is fixed and the weighted adjacency matrix A is positive constant and given. Moreover, $a_{ii}=0$, for $i=1, \cdots, N$. (2) There is no time delay and packet dropouts when data is transferred from ith DG to its local controller, vice versa; the delay of data transmission from the ith DG to the jth DG via networks is bounded by s_{ij} and the number of its consecutive data loss is bounded

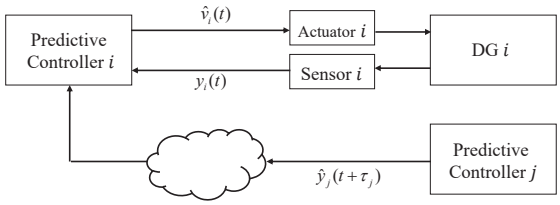

Fig. 2. Communication structure of the Microgrid

by ρ_{ij}, all data transmitted through networks are timestamped. (3) The controller clocks of all distributed generation units are synchronized. (4) The desired reference values are only available for some power generation units, i.e, only for the pinning nodes. Let $\tau_j{=}\rho_{ji}{+}s_{ji}$, where both ρ_{ji} and s_{ji} are an integer multiple of the sampling period of the practical system guaranteeing τ_j is a positive integer number. The islanded microgrid to be investigated, with the communication structure described above, is shown as Fig. 2. In summary, the main contribution of this paper is to solve the voltage restoration problem of microgrids with communication constraints by a pining-based distributed predictive control method of secondary voltage.

3. DYNAMICAL MODEL OF INVERTER-BASED DG

Since transient dynamics of power electronics are fast enough in comparison with slow variations in voltage amplitude and/or phase of phasor variables in MG, modeling a MG system dynamics from droop-control is sufficient for voltage restoration problems. For highly inductive transmission lines (if the inductive part is the dominant one among reactance) of reactance X_{ij} connecting DG_i to DG_j, the real and reactive power P_i and Q_i can be obtained as follows (Weckx et al., 2015)

$$P_i = \sum_{j=1}^{N} \frac{V_i V_j}{X_{ij}} \sin(\theta_i - \theta_j),$$
$$Q_i = \sum_{j=1}^{N} \frac{V_i^2}{X_{ij}} + \sum_{j=1}^{N} \frac{V_i V_j}{X_{ij}} \cos(\theta_i - \theta_j)$$

where V_i, θ_i are the voltage RMS values and phase angle of DG_i, respectively, and V_j, θ_j have the same meaning. For transient stability of the whole system, $\theta_{ij}{=}\theta_i{-}\theta_j$ is small (Machowski et al., 1997), then above equation can be approximated as

$$P_i = \sum_{j=1}^{N} \frac{V_i V_j}{X_{ij}} \theta_{ij},\ Q_i = \sum_{j=1}^{N} \frac{V_i^2}{X_{ij}} + \sum_{j=1}^{N} \frac{V_i V_j}{X_{ij}}. \quad (1)$$

It can be concluded from the above equation that in the inductive dominated microgrid system, the reactive power transmitted from DG_i to DG_j is strongly coupled with the voltage magnitude, so the reactive power transmission from DG_i to DG_j can be controlled by adjusting the voltage magnitude, which is the traditional droop control scheme. To maintain the voltage, the reactive power droop control can be obtained as follows $v_{odi}{=}V_{ni}{-}n_iQ_i(t), v_{oqi}{=}0$, where V_{ni} is the nominal voltage value serving as the input of the primary control loop, Q_i is the measured reactive power values of DG_i, correspondingly n_i is the reactive droop gain which can be given based on the inverter ratings. From equation above, it's not difficult to get the voltage magnitude $v_{o,magn}{=}\sqrt{v_{odi}^2{+}v_{oqi}^2}{=}v_{odi}$. So, the equation (1) can be rewritten as

$$v_{o,magn} = V_{ni} - n_i Q_i(t). \quad (2)$$

Similarly, active power droop characteristics can be applied to tune the frequency of inverter by the following equation

$$\omega_i(t) = \omega_{ni} - m_i P_i(t). \quad (3)$$

Thus, considering the dynamics of the coupling connector connecting the DGs, the dynamics of output LC filter, and the droop characteristics (2) and (3), denote v_{odi} and v_{ni} as the output and input variables, respectively. Then the large-signal model of distributed generation unit based on inverter can be obtained as follows

$$\begin{cases} \dot{x}_i(t) = f_i(x_i(t)) + k_i(x_i(t))D_i + g_i(x_i(t))u_i(t) \\ y_i(t) = v_{odi} = C_i x_i(t) \end{cases}$$

where state variables $x_i(t){=}[\ P_i\ \ Q_i\ \ i_{Ldi}\ \ i_{Lqi}\ \ v_{odi}\ \ v_{oqi}\ \ i_{odi}\ \ i_{oqi}\ ]^T$. The term $D_i = \begin{bmatrix} v_{bdi} & v_{bqi} \end{bmatrix}^T$ is considered as a known disturbance. For secondary voltage control, the large-signal model can be linearized as the following linear model

$$\begin{cases} \dot{x}_i(t) = A_i x_i(t) + B_i u_i(t) \\ y_i(t) = v_{odi} = C_i x_i(t). \end{cases}$$

The detailed expressions for $f_i(x_i)$, $k_i(x_i)$, $g_i(x_i)$, A_i, B_i, C_i are adopted from the nonlinear model proposed in Pogaku et al. (2007). Further, according to Euler's discretization formula, the above system can be written as the following discrete linear system

$$\begin{cases} \dot{\zeta}_{id}(k+1) = A_{id}\zeta_{id}(k) + B_{id}v_i(k) \\ y_i(k) = C_{id}\zeta_{id}(k). \end{cases} \quad (4)$$

4. PINING-BASED DISTRIBUTED PREDICTIVE SECONDARY VOLTAGE CONTROLLER

4.1 Output prediction and optimal design of the controller

To design the pinning-based predictive voltage controller, the cost function $J_i(t)$ of the DG_i is proposed as

$$\begin{aligned} J_i = & d_i \sum\nolimits_j a_{ij} \left\| \hat{Y}_j(t+N_y|t-\tau_j) - \hat{Y}_i(t+N_y|t) \right\|^2 \\ & + g_i \left\| Y_i^* - \hat{Y}_i(t+N_y|t) \right\|^2 + c_i \left\| \hat{V}_i(t+N_u|t) \right\|^2 \end{aligned} \quad (5)$$

where,

$$\begin{aligned} & Y_i^* = V_i^{ref}(t) I_N, \\ & \hat{V}_i(t+N_u|t) = [\ \hat{v}_i(t+N_u|t)\ \cdots\ \hat{v}_i(t|t)\ ]^T, \\ & \hat{Y}_i(t+N_y|t) = [\ \hat{y}_i(t+N_y|t)\ \cdots\ \hat{y}_i(t+1|t)\ ]^T, \\ & \hat{Y}_j(t+N_y|t-\tau_j) = [\ \hat{y}_j(t+N_y|t-\tau_j)\ \ \cdots \\ & \qquad\qquad \hat{y}_j(t+1|t-\tau_j)\ ]^T, \end{aligned}$$

I_N denotes the N dimensional all-ones vector and the integers N_y and N_u are the prediction horizon lengths of the outputs and control inputs, respectively, d_i and c_i are weighting factors, a_{ij} is the (i,j)th element of adjency matrix that determines the network topology of MG, and g_i is the pinning control gain. The local cost function $J_i(t)$ of designing the secondary predictive controller is composed of three parts. First-term considers the voltage difference between the output predictions of the DG_i and each neighboring DG_j for a certain period of time with the length of N_y, which represents the coordination performance of the DGs. The second term considers the

voltage difference between the output predictions of the pinning DG_i and the reference voltage of MG, which represents the tracking performance of the DG_i, i.e. $g_i \neq 0$. The last term is about the constraint on the control input ensuring that the control inputs are feasible in a real power system.

The optimal solution of the prediction term V_i is to minimize the cost function $J(t)$, where $J=\sum_{i=1}^{N} J_i$. So the primary task is to obtain the prediction output vectors appeared in cost function (5). First, following the idea in Liu (2017), a multi-step predictor of the state vector for DG_i is proposed as follows.

(1) State prediction from t to $t+N_u$

$$\hat{\zeta}_i(t+k|t) = A_{id}\hat{\zeta}_i(t+k-1|t) + B_{id}\hat{v}_i(t+k-1|t)$$

where $k = 1, \cdots, N_u$. Employing the above equation recursively yields

$$\hat{\zeta}_i(t+k|t) = A_{id}^{k}\zeta_i(t) + \sum_{l=1}^{k} A_{id}^{k-l}B_{id}\hat{v}_i(t+l-1|t).$$

(2) State prediction from $t+N_u+1$ to $t+N_y+\tau_j$

$$\hat{\zeta}_i(t+k|t) = A_{id}\hat{\zeta}_i(t+k-1|t) + B_{id}\hat{v}_i(t+k-1|t)$$

where $k = N_u+1, \cdots, N_y+\tau_j$. When the DG_i control inputs are beyond the control horizon length, let $\hat{V}_i(t+k|t)=\hat{V}_i(t+N_u|t), k>N_u$. Then, employing the above equation recursively yields

$$\hat{\zeta}_i(t+k|t)=A_{id}^{k}\hat{\zeta}_i(t+N_u|t) + \sum_{l=1}^{k} A_{id}^{k-l}B_{id}\hat{v}_i(t+N_u+l-1|t).$$

Then, based on the state vector predictions above, the output predictions of the DG_i can be obtained by

$$\hat{y}_i(t+k|t) = C_i\hat{\zeta}_i(t+k|t) \tag{6}$$

where $k = 1, \cdots, N_y$. So, the following prediction vector can be obtained from (6)

$$\hat{Y}_i(t+N_y|t) = M_i\zeta_i(t) + F_i\hat{V}_i(t+N_u|t) \tag{7}$$

where

$$M_i = \begin{bmatrix} C_{id}A_{id}^{N_y} & \cdots & C_{id}A_{id}^{N_u+1} & C_{id}A_{id}^{N_u} & \cdots & C_{id}A_{id}^{1} \end{bmatrix}^T,$$

$$F_i = \begin{bmatrix} \sum_{l=1}^{N_y-N_u} C_{id}A_{id}^{N_y-N_u-l}B_{id} & C_{id}A_{id}^{N_y-N_u}B_{id} & \cdots & C_{id}A_{id}^{N_y-1}B_{id} \\ \vdots & & \ddots & \vdots \\ C_{id}B_{id} & C_{id}A_{id}^{1}B_{id} & \cdots & C_{id}A_{id}^{N_u}B_{id} \\ 0 & C_{id}B_{id} & \cdots & C_{id}A_{id}^{N_u-1}B_{id} \\ \vdots & & \ddots & \vdots \\ 0 & 0 & \cdots & C_{id}B_{id} \end{bmatrix}.$$

Similarly, the output predictions based on data from $t-\tau_j$ are

$$\begin{aligned} \hat{Y}_j(t+N_y|t-\tau_j) &= M_{ji}\zeta_i(t) + F_{ji}\hat{V}_i(t+N_u|t) \\ &= I_{\tau_j}(\bar{M}_i\zeta_i(t) + \bar{F}_i\hat{V}_i(t+N_u|t)) \end{aligned} \tag{8}$$

where $I_{\tau_j}=\begin{bmatrix}0_{N_y\times\tau_j} & I_{N_y\times\tau_j}\end{bmatrix}$, $\bar{M}_i=\begin{bmatrix}M_i' & M_i\end{bmatrix}^T$, $\bar{F}_i=\begin{bmatrix}F_i' & F_i\end{bmatrix}^T$,

$$M_{i'} = \begin{bmatrix} C_{jd}A_{jd}^{\tau_j+N_y} & \cdots & C_{jd}A_{jd}^{N_y+1} \end{bmatrix}^T,$$

$$F_i' = \begin{bmatrix} C_{jd}(\sum_{l=1}^{N_y-N_u} A_{jd}^{\tau_j+N_y-N_u-l} + \sum_{L=1}^{\tau_j} A_{jd}^{\tau_j-L})B_{jd} \\ \vdots \\ C_{jd}(\sum_{l=1}^{N_y-N_u} A_{jd}^{k+N_y-N_u-l} + \sum_{L=1}^{k} A_{jd}^{k-L})B_{jd} \\ \vdots \\ C_{jd}(\sum_{l=1}^{N_y-N_u} A_{jd}^{1+N_y-N_u-l} + \sum_{L=1}^{1} A_{jd}^{1-L})B_{jd} \end{bmatrix}$$

$$\begin{bmatrix} C_{jd}A_{jd}^{\tau_j+N_y-N_u}B_{jd} & C_{jd}A_{jd}^{\tau_j+N_y-N_u+1}B_{jd} & \cdots & C_{jd}A_{jd}^{\tau_j+N_y-1}B_{jd} \\ \ddots & & & \\ C_{jd}A_{jd}^{k+N_y-N_u}B_{jd} & C_{jd}A_{jd}^{k+N_y-N_u+1}B_{jd} & \cdots & C_{jd}A_{jd}^{k+N_y-1}B_{jd} \\ \ddots & & & \\ C_{jd}A_{jd}^{1+N_y-N_u}B_{jd} & C_{jd}A_{jd}^{1+N_y-N_u+1}B_{jd} & \cdots & C_{jd}A_{jd}^{1+N_y-1}B_{jd} \end{bmatrix}.$$

Now, the designed optimal predictive voltage control V_i for $i = 1, \ldots, N$ can be derived by minimizing the global cost function, which implies

$$\frac{\partial}{\partial \hat{V}_i(t+N_u|t)} \sum_{i=1}^{N} J_i(t) = 0$$

i.e.

$$\begin{aligned} &-d_iF_i^T(\sum_j a_{ij}(\hat{Y}_j(t+N_y|t) - \hat{Y}_i(t+N_y|t))) \\ &-g_iF_i^T(Y_i^* - \hat{Y}_i(t+N_y|t)) + c_i\hat{V}_i(t+N_u|t) = 0. \end{aligned}$$

Then, substituting the output prediction vectors (7) in the above equation leads to

$$\begin{aligned} &-F_i^T\sum_j a_{ij}(\hat{Y}_j(t+a_i+N_y|t-\tau_{ji}) - M_i\hat{\zeta}_i(t-\tau_i|t-\tau_i-1) \\ &-F_i\hat{V}_i(t+a_i+N_u|t-\tau_i)) + g_iF_i^T(M_i\hat{\zeta}_i(t-\tau_i|t-\tau_i-1) \\ &+F_i\hat{V}_i(t+a_i+N_u|t-\tau_i) - Y_i^*) + c_i\hat{V}_i(t+N_u|t-s_i) = 0. \end{aligned}$$

As a result, it can be calculated from the above equation that the optimal solution is

$$\begin{aligned} \hat{V}_i(t+N_u|t) = \Gamma_i^{-1}(&F_i^T\sum_j a_{ij}\hat{Y}_j(t+N_y|t-\tau_j) + g_iF_i^TY_i^* \\ &- (F_i^TM_i\sum_j a_{ij} + g_iF_i^TM_i)\hat{\zeta}_i(t|t-1)) \end{aligned}$$

where $\Gamma_i = (F_i^TF_i\sum_j a_{ij} + g_iF_i^TF_i + c_iI)$.

Adjusting the weighting factors can guarantee that the matrix Γ_i is invertible. Lastly, the pinning-based secondary voltage predictive control of DG_i at time t is given as follows

$$\hat{v}_i(t) = H_{v,i}\hat{V}_i(t+N_u|t) \tag{9}$$

where $H_{v,i} = \begin{bmatrix} 0 & \cdots & 0 & \cdots & 1 \end{bmatrix}$.

4.2 The pinning-based distributed predictive control scheme

The implementation of a pinning-based distributed predictive secondary voltage control scheme can be divided into two steps. In the first step, the linear state-space description of the system is obtained by the small disturbance linearization of the large-signal model of the microgrid, then the discrete linear system can be derived by Euler discretization. In the second step, the prediction control input at time t is calculated by (9), which will minimize the global cost function, which is the sum of (5) for $i = 1, \cdots, N$. This part plays a key role in tracking the prescribed reference based on the performance of the pining DG and the coordination between the DGs through information exchange, which will guarantee the voltage restoration of microgrid via tuning the weighting factors in the cost function. The control scheme proposed can be comprehensively summarized by Fig.3.

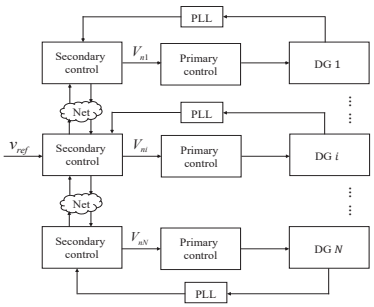

Fig. 3. The algorithm structure of the secondary voltage predictive control ($g_i \neq 0$)

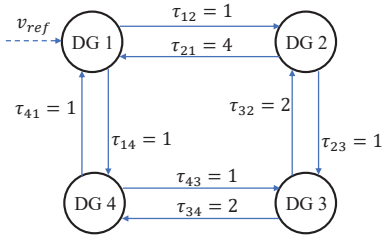

Fig. 4. The communication structure of the test MG under secondary voltage predictive control ($g_1 \neq 0$)

In order to analyze the stability of the MG system, an operator Δ is defined to be $\Delta x(t) = x(t) - x(t-1)$ for $x(t)$, and the prediction error is defined as $e(t) = \zeta_{id}(t) - \hat{\zeta}_{id}(t|t-1)$. Using the state prediction vector, the output prediction vector (7) and the prediction control (9), a closed-loop system with zero input and state vector $\varsigma(t) = [\,\Delta\zeta_{id}(t)\ \Delta e(t)\,]^T$ can be obtained. Therefore, the necessary and sufficient condition of stability of the MG system is that the system matrix of the closed-loop system is Schur stable. The detailed proof process is similar to Liu (2018), which will be given in future studies, and omitted here for limited space.

5. SIMULATION RESULTS

To validate the effectiveness of the proposed secondary predictive control approach, we have considered a typical MG architecture with four DGs. The network communication delays are assumed to be $\tau_{12} = \tau_{41} = \tau_{43} = \tau_{23} = 1$, $\tau_{32} = 2, \tau_{34} = 2$, $\tau_{21} = 4$. And, the DG_1 is selected as the pinning node such that it can directly receive the reference value. Therefore the weighting factors $g_1 \neq 0$, while it will be 0 for other nodes in (5). The cyber layer of the test MG system with the above time delays is shown in Fig. 4. It is worth mentioning that the communications among the DGs are all bidirectional. Although the reference voltage cannot be directly obtained by nodes rather than the pining node, the synchronization of all DGs can be achieved through network communication under the proposed control method. For simplicity, it is assumed that the predictive secondary voltage control is on operation at the beginning and each DG has initial deviation caused by the droop control. In the simulation, the initial voltage magnitude of DG_1 to DG_4 are chosen as 0.90, 0.92, 0.91, and 0.93 p.u.. Three simulation cases are carried out: one is that voltage control results using predictive control (PC) with coordination and without coordination, another one is voltage control results using PC with coordination under

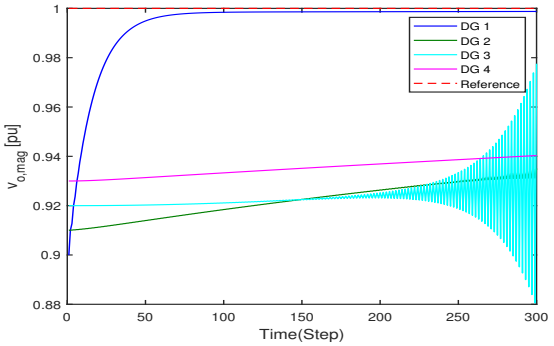

Fig. 5. DGs output voltage without coordination

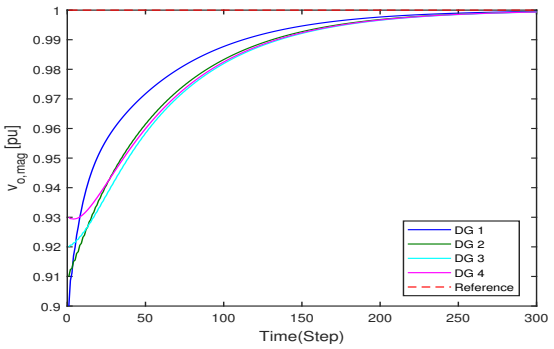

Fig. 6. DGs output voltage with coordination

various weighting factors, the last one is voltage control results using PC with coordination under the different reference voltage values.

Case 1: Voltage control results using PC with coordination and without coordination. The simulated four DGs voltage output responses of the individual control islanded MG without coordination ($d_i = 0$ for all $i \in V_g$) are shown in Fig. 5. It is clear from the simulations that only the voltage of the pining node DG_1 realizes the restoration to the reference value, while the other DGs do not realize voltage tracking, which will cause the failure of grid-connection. This is mainly because there is no information exchange among the four DGs, so other DGs cannot access to the reference voltage indirectly. To achieve the goal that the voltage of all DGs in a MG will restore to the rated level, they have to exchange their operation information. Based on the assumption above, the communication network is shown in Fig. 4. The parameters of the cost function (5) are set to be as follows: $N_y = 15$, $N_u = 14$, c_i=5, $d_i = 0.3$, for all $i \in V_g$, and $g_1 = 0.3$. The developed pining-based secondary voltage controller (9) is utilized. The simulated voltage outputs of the four DGs are shown in Fig. 6 and the corresponding control inputs of the DGs are shown in Fig. 7. The simulation results clearly illustrate that the four DGs have realized the voltage restoration and have been the similar transient output responses, which is consistent with the theoretical analysis.

Case 2: Voltage control results using PC with coordination under the different weighting factors. The cost function J_i defined in (5) is designed to make it as small as possible. It is clear that the weighting factors d_i, g_i, and c_i will influence the output response of the controller explicitly. Generally speaking, for better control performance, it demands a larger d_i, g_i and a smaller c_i to keep J small. To show the

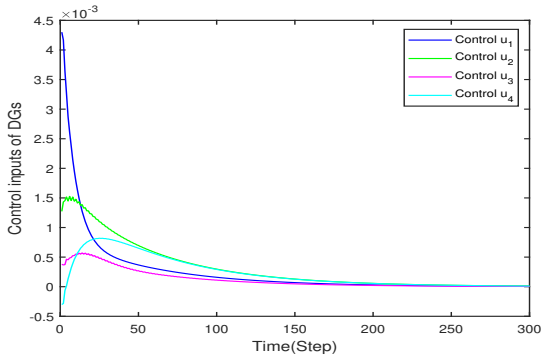

Fig. 7. The control inputs of DGs with coordination

effect of weighting factors on the output response speed and tracking performance, two set weighting factors are considered, i.e. $c_i = 5$, for all $i \in V_g$, $d = [0.2, 0.4, 0.8, 1.2]$, $g_1 = 0.5$ and $c_i = 5$, $d_i = 0.1$, for all $i \in V_g$, $g_1 = 0.2$. In the two cases, the reference voltage is chosen as the same, i.e. $v_{ref} = 1$ p.u. and the simulation results are shown in Fig. 8. Comparing case 1 shown in Fig. 8 (a) with case 2 shown in Fig. 8 (b), it can be concluded that the output voltage magnitudes of DG with a larger c_i in its secondary predictive voltage controller will converge to reference voltage faster than one has a smaller c_i in its controller.

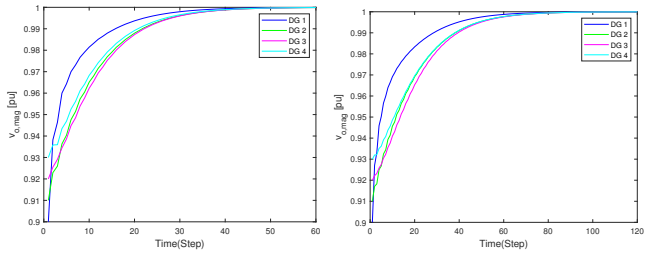

(a) (b)

Fig. 8. DGs output voltage magnitudes response with the following weighting factors: (a) $d = [0.2, 0.4, 0.8, 1.2]$, $g_1 = 0.5$, (b) $d = [0.1, 0.1, 0.1, 0.1]$, $g_1 = 0.2$.

Case 3: Voltage control results using PC with coordination under the different reference values (1.05, 0.95 p.u). In this case, to verify the proposed pining-based predictive voltage controller is robust to the reference value, Fig. 9 illustrates the voltage amplitudes response when the reference value is set to 0.95 and 1.05 p.u. The remained controller parameters in this situation are chosen as the same as the coordination subclass in Case 1. As seen, the secondary control restores all DG terminal voltage amplitudes to the pre-specified reference.

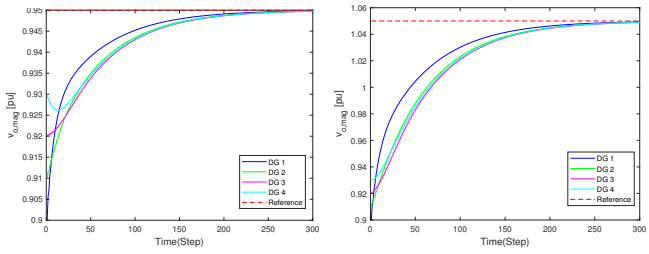

(a) (b)

Fig. 9. DGs output voltage magnitudes for different reference voltage: (a) $v_{ref} = 0.95$p.u., (b) $v_{ref} = 1.05$p.u..

6. CONCLUSION

In this paper, the concept of distributed pining-based predictive control is proposed and adopted successfully to implement the secondary voltage control of microgrid where there exist network delays and packet dropouts. The controller for each DG is fully distributed and could actively compensate for the network delays and data loss, in which just pining DG can directly achieve the reference voltage. And only the information of each DG and that of its neighbors are required for the controller. To validate the proactivity of the proposed control scheme, a microgrid with four DGs taking network communication delays and packet dropouts into consideration is used. The simulation results also show that the proposed approach has better synchronization speed via tune the controller parameters appropriately.

REFERENCES

Aryani, D.R. and Song, H. (2019). Voltage regulation in a stand-alone dc microgrid. *IFAC-PapersOnLine*, 52(4), 36 – 39. IFAC Workshop on Control of Smart Grid and Renewable Energy Systems CSGRES 2019.

Bidram, A., Davoudi, A., Lewis, F.L., and Guerrero, J.M. (2013). Distributed cooperative secondary control of microgrids using feedback linearization. *IEEE Transactions on Power Systems*, 28(3), 3462–3470.

Guerrero, J.M., Vasquez, J.C., Matas, J., de Vicuna, L.G., and Castilla, M. (2011). Hierarchical control of droop-controlled ac and dc microgrids—a general approach toward standardization. *IEEE Transactions on Industrial Electronics*, 58(1), 158–172.

Lai, J., Lu, X., and Yu, X. (2019). Stochastic distributed frequency and load sharing control for microgrids with communication delays. *IEEE Systems Journal*, 1–12.

Liu, G. (2017). Predictive control of networked multiagent systems via cloud computing. *IEEE Transactions on Cybernetics*, 47(8), 1852–1859.

Liu, G. (2018). Predictive control of networked nonlinear multiagent systems with communication constraints. *IEEE Transactions on Systems, Man, and Cybernetics: Systems*, 1–11.

Lu, X., Lai, J., Yu, X., Wang, Y., and Guerrero, J.M. (2018). Distributed coordination of islanded microgrid clusters using a two-layer intermittent communication network. *IEEE Transactions on Industrial Informatics*, 14(9), 3956–3969.

Machowski, J., Bialek, J., Bumby, J., and Bumby, J. (1997). *Power System Dynamics and Stability*. Wiley.

Pogaku, N., Prodanovic, M., and Green, T.C. (2007). Modeling, analysis and testing of autonomous operation of an inverter-based microgrid. *IEEE Transactions on Power Electronics*, 22(2), 613–625.

Weckx, S., D'Hulst, R., and Driesen, J. (2015). Primary and secondary frequency support by a multi-agent demand control system. *IEEE Transactions on Power Systems*, 30(3), 1394–1404.

Zhang, R. and Hredzak, B. (2019). Distributed finite-time multiagent control for dc microgrids with time delays. *IEEE Transactions on Smart Grid*, 10(3), 2692–2701.

Zhong, Q. and Weiss, G. (2011). Synchronverters: Inverters that mimic synchronous generators. *IEEE Transactions on Industrial Electronics*, 58(4), 1259–1267.